ACS Sustainable Resource Management

pubs.acs.org/acssrm

Article

Unveiling Dissolution Kinetics of CuO Nanofertilizer Using Bio-Based Ionic Liquids Envisaging Controlled Use Efficiency for Sustainable Agriculture

Mónia A. R. Martins, Leonard M. Kiirika, Nicolas Schaffer, Adam Sajnóg, João A. P. Coutinho, Gregory Franklin,* and Dibyendu Mondal*

Cite This: *ACS Sustainable Resour. Manage.* 2024, 1, 1291−1301

Read Online

ACCESS | Metrics & More | Article Recommendations | Supporting Information

ABSTRACT: The need for sustainable agriculture amid a growing population and challenging climatic conditions is hindered by the environmental repercussions of widespread fertilizer use, resulting in the accumulation of metal ions and the loss of micronutrients. The present study provides an approach to improve the efficiency of nanofertilizers by controlling the release of copper (Cu) ions from copper oxide (CuO) nanofertilizers through bioionic liquids based on plant growth regulators (PGR-ILs). A 7-day study was conducted to understand the kinetics of Cu ion release in aqueous solution of five different PGR-ILs, with choline ascorbate ([Cho][Asc]) or choline salicylate ([Cho][Sal]) leading to 200- to 700-fold higher dissolution of Cu ions in comparison to choline indole-3-acetate ([Cho][IAA]), choline indole-3-butyrate ([Cho][IBA]), and choline gibberellate ([Cho][GA_3]). The tunable diffusion of Cu ions from CuO nanofertilizers using PGR-ILs is then applied in a foliar spray study, evaluating its impact on the growth phenotype, photosynthetic parameters, and carbon dioxide (CO_2) sequestration in *Nicotiana tabacum* in a greenhouse. The results indicate that nanoformulations with lower concentrations of Cu ions in PGR-IL solutions exhibit superior outcomes in terms of plant length, net photosynthetic rate, dry biomass yield, and CO_2 sequestration, emphasizing the critical role of dissolution kinetics in determining the effectiveness of PGR-IL-based nanoformulations for sustainable agriculture.

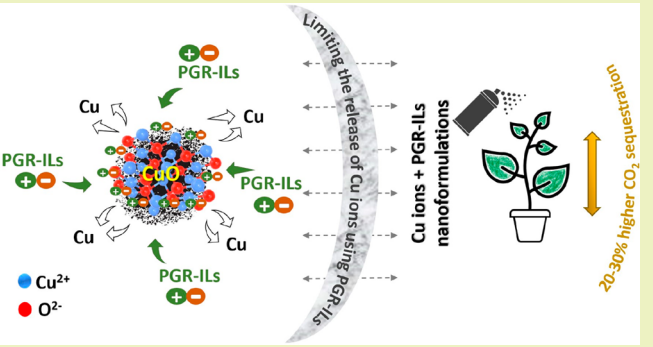

KEYWORDS: *Bio-ionic liquids, Copper oxide, Nanoformulation use efficiency, Ion release kinetics, Nanoparticles, Nicotiana tabacum*

INTRODUCTION

In the face of global population growth, the concept of sustainable agriculture and food security is becoming increasingly important. It is estimated that food production needs to increase 50−80% by 2050.[1] Among the ineffective practices, the use of fertilizers in agriculture is a major problem because only about 30% of fertilizers are utilized by crops, resulting in unnecessary waste of energy, water, and arable land.[2,3] Therefore, novel agricultural strategies are being sought, and among these, tailored nanomaterials (NMs) stand out as sustainable alternatives because they have the potential to control the release of nutrients and stimulate plant defenses against biotic (such as pests and pathogens) and abiotic stresses (such as drought, salinity, temperature, etc.).[4] Micronutrients play an important role in plant response to diseases, as they are able to defense plant from pathogens.[5] Usually, micronutrients are applied to crops in the form of salts or hydroxides.[6,7] Although on one hand this approach is quite effective, on the other hand one must be careful with the possible accumulation of metals in soils and sediments and leaching into watercourses.[8,9] Moreover, the availability of micronutrients in soil is limited and foliar applications are quite ineffective for many pathogens due to the limited transfer of nutrients from leaves to roots.[6] In this sense, NMs represent an interesting micronutrient delivery system due to their large surface area and the fact that their properties such as shape and composition can be tuned to optimal conditions.[2,4,10] Among the nanoscale micronutrients currently under investigation, metals and metal oxides stand out due to their increased availability and translocation in plants.[10] In addition to enhanced nutrient uptake, nanoformulations of metal oxides, such as copper oxide (CuO) and iron oxide (Fe_2O_3), are known for their effectiveness in mitigating disease damage.[2,11]

Received: February 1, 2024
Revised: April 2, 2024
Accepted: April 24, 2024
Published: May 8, 2024

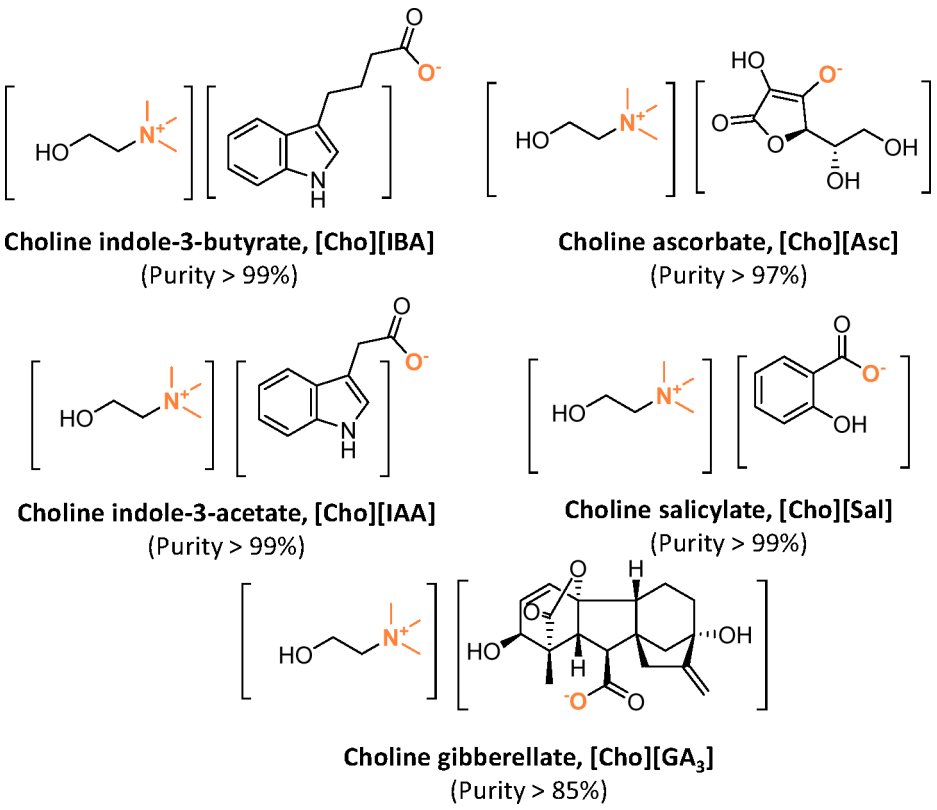

Figure 1. Name, abbreviation, chemical structure, and mass fraction purity (% determined by ^{1}H NMR (Figure S1)) of synthesized PGR-ILs.

The interaction of engineered NMs with plants is influenced by several factors, including their size, shape, surface charge, stability, solubility, and controlled release profile.[12] These properties of NMs can promote plant defense, stimulate the production of secondary metabolites, and ensure cost-effectiveness for sustainable agricultural practices.[6,11,13] Studies on the structural and surface properties of NMs and their beneficial effects on plant growth, productivity, and gene delivery have been reported.[14,15] However, studies addressing the dissolution effect of NMs on micronutrient use efficiency and controlling plant growth are scant. Borgatta et al.[6] demonstrated that Cu-based NMs were able to suppress *Fusarium* infections in watermelon and increase yield. Later, Ma et al.[2] investigated the morphology, composition, and dissolution of various Cu-based micronutrients capable of suppressing sudden death syndrome in soybeans. Both papers[2,6] evaluated ion release profiles and attempted to control the release of Cu ions from NMs using surfactants and simulated xylem sap solutions. In addition, Cu-based NMs may exhibit dual functionality: at low concentrations, they promote plant growth, while at high concentrations they inhibit overall plant development due to the formation of excessive reactive oxygen species.[16] Therefore, it is important to understand the release kinetics of Cu ions from CuO nanoparticles (NPs) to improve the effectiveness of NM-based formulations. In this article, we propose for the first time the suitability of ionic liquids based on plant growth regulators (PGR-ILs) for the controlled release of metal ions from NMs, envisaging agricultural applications.

ILs are a well-known class of green solvents whose structures can be tailored according to the desired properties and are therefore used in various fields.[17] These neoteric solvents are known for their excellent abilities in extracting and dissolving various types of compounds from biological resources.[18] PGR-ILs represent an innovative approach in agricultural science, where the unique properties of ILs are shaped to influence and enhance plant growth. Those are typically composed of the choline precursor which is commonly found in plant tissues and naturally derived anions such as plant growth hormones like indole-3-acetic acid or gibberellic acid. The resulting ionic compounds offer a controlled and sustained release of PGRs, creating a targeted delivery system that optimizes their efficiency while minimizing environmental impact, as these compounds are biodegradable and non-toxic. DNA was previously solubilized and successfully preserved in choline indole-3-acetate IL.[19]

The present study primarily aims to investigate the dissolution kinetics of Cu ions from CuO in aqueous solutions containing bio-based PGR-ILs composed of biomolecules derived from PGRs. CuO was selected because it is widely used as nanofertilizers, plant protectant, and nanozymes to mitigate plant stress.[20] In addition, aqueous nanoformulations of PGR-ILs and dissolved Cu ions were administered to *Nicotiana tabacum* (tobacco) plants in a greenhouse to assess the impact of NPs on the growth phenotype, photosynthetic parameters, and CO_2 sequestration. Overall, the formulation with fewer Cu ions led to improved plant growth parameters. It is expected that the results of this research will contribute to the further development and understanding of various mechanisms associated with NMs in the field of plant nanotechnology to achieve progress in sustainable agriculture.

MATERIALS

Choline bicarbonate (80% w/w aqueous solution, Sigma), ascorbic acid (99.7%, Sigma-Aldrich), indole-3-acetic acid (98%, Alfa Aesar), indole-3-butyric acid (98%, Alfa Aesar), gibberellic acid (>98%, TCI),

https://doi.org/10.1021/acssusresmgt.4c00041
ACS Sustainable Resour. Manage. 2024, 1, 1291−1301

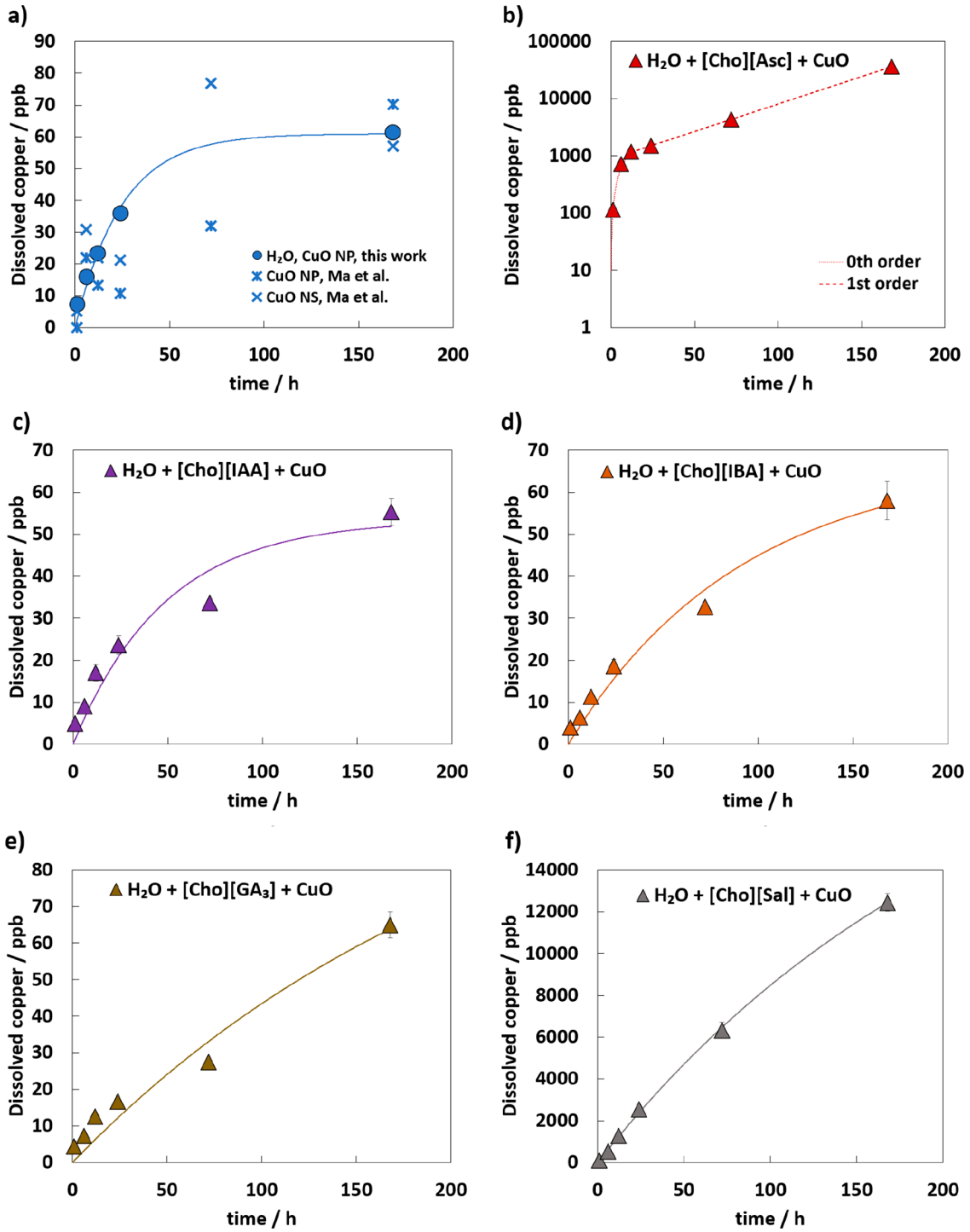

Figure 2. Time-dependent dissolution of Cu ions from commercial CuO NPs in different systems at 25°C and at an initial mass concentration of approximately 100 mg/L (see Table S1 for exact values). Panel (a) shows a comparison with data from Ma et al.[2] in CuO NP and nanosheets (NS). Plots (b)−(f) show dissolution kinetics of Cu ion in the aqueous solutions of [Cho][Asc], [Cho][IAA], [Cho][IBA], [Cho][GA_3], and [Cho][Sal], respectively.

and salicylic acid (99%, Acofarma) were used without further purification to synthesize the PGR-ILs. Figure 1 shows comprehensive details about the ILs and their corresponding chemical structures. Ultrapure water was double distilled, passed through a reverse osmosis system, and further treated with a Milli-Q plus 185 water purifier (resistivity = 18.2 MΩ cm, total organic content <5 μg dm^{-3}, free of particles >0.22 μm). CuO nanopowder water dispersion (CuO, 99.95%, 25−55 nm, 20 wt % in water, stock# US7566, CuO CAS# 1317-38-0, H_2O CAS# 7732-18-5) was purchased from US Research Nanomaterials, Inc (USA). The NPs were homogenized and freeze-dried before use. Analytical grade ethanol was purchased from Fisher Scientific, and dialysis tubing cellulose membranes were purchased from Sigma (D9277). Additional experimental details are described in the Supporting Information (SI). The composition of each system, in terms of IL and CuO concentrations, is listed in Tables S1 and S2 for the ion release profile and plant application experiments, respectively.

https://doi.org/10.1021/acssusresmgt.4c00041
ACS Sustainable Resour. Manage. 2024, 1, 1291−1301

RESULTS AND DISCUSSION

Effect of PGR-ILs on the Cu Ion Release Kinetics from CuO Nanofertilizer. Like most metal oxides, CuO has a packed crystal structure and thus high lattice energies (U_{CuO} = 4050 kJ mol^{-1}) due to the small distances between the oxygen anion and the Cu cation,[21] which makes it a very stable compound and leads to low dissolution. Another useful thermodynamic parameter that helps in estimating stability is the Gibbs energy of formation ($\Delta G^0_{f,CuO}$ = −128.4 kJ mol^{-1});[22] more stable compounds have a smaller value of ΔG^0_f. However, other factors, such as variations in speciation, coordination numbers of metal ions, and the presence of foreign ligands that determine the tendency for ion release of CuO, are also important. Previous studies have shown that the release of Cu ions from CuO-based NMs can be tuned using surfactants and simulated xylem sap solutions containing sugars and organic acids such as succinic acid, fumaric acid, and malic acid.[2,6,23] However, the detailed dissolution kinetics of CuO NPs are not discussed. In this article, we investigate the suitability of PGR-ILs containing various PGRs and signaling molecules to control the dissolution kinetics of CuO NPs and decipher the potential of PGR-ILs to fine-tune the CuO nanoformulations' use efficiency.

The release profiles of Cu ions were studied using cellulose membranes in dialysis tubes, as described in the experimental section available in the SI.[24] The main advantage of this technique is that it avoids the sampling of undissolved solutes dispersed in the aqueous phase, an experimental error that can lead to overestimated values. With a molecular weight cut-off of 14 kDa, the dialysis tubing used in the present study is recommended to retain particles with a molecular weight of 12 kDa or more.[25] Dissolution of Cu ions from CuO in pure water was used to validate the method by comparing the results to values from the literature (Figure 2a). The results agree well with the data of Ma et al.[2] for the dissolution of CuO NPs and nanosheets (NS) in deionized water, where the authors used an initial equivalent Cu molar concentration of 0.69 mM and ultrafiltration centrifugal filter units (3 kDa). However, it is important to emphasize that the time dependence of the release of Cu ions from CuO strongly depends on the initial NP concentration, the morphology of CuO, and the dissolution medium.[26] In addition, an attempt was made to use only centrifugation (15000 rpm, 30 min) as a separation technique. However, this proved to be inefficient and resulted in overestimated dissolved Cu values (Cu ions >0.5 mg/L, after 19 h), as observed in the work of Borgatta et al.[6]

Figure 2a−f shows the dissolution kinetics results of CuO NPs in water and in different aqueous media comprising [Cho][Asc], [Cho][IAA], [Cho][IBA], [Cho][GA_3], and [Cho][Sal]. The data of Figure 2 are listed in Table S3. The Cu dissolution data obtained were described, whenever possible, by a modified first-order reaction rate eq 1:[24]

$$D(t) = D_f(1 - e^{-kt}) \quad (1)$$

where $D(t)$ is the released amount of Cu (μg/L), D_f is the final steady-state concentration of the released Cu, k is the rate coefficient (h^{-1}), and t the time (h). Both constants, D_f and k, were determined by fitting the experimental data and are provided in Table 1. NPs are characterized by a rapid initial release of ions across the different media investigated and exhibit continuous particle dissolution over the 1-week period evaluated. An initial logarithm analogous behavior is observed but without reaching a plateau within the measuring time, except for water where a nearly constant value was reached after 100 h (final dissolution, $D_{f,CuO\ in\ H_2O}$ = 61 μg/L). The rate coefficient of the dissolution curve follows the order of k_{H_2O} (0.040 h^{-1}) > $k_{H_2O+[Cho][IAA]}$ (0.021 h^{-1}) > $k_{H_2O+[Cho][IBA]}$ (0.011 h^{-1}) > $k_{H_2O+[Cho][Sal]}$ = (0.004 h^{-1}) = $k_{H_2O+[Cho][GA3]}$ (0.004 h^{-1}), which further highlights the difference in the dissolution behavior between the different media used. The presence of [Cho][Asc] in solution alters the kinetic trend, precluding the use of eq 1 to describe the experimental data. In this system, data were adjusted using a two-step process with 0th- and 1st-order equations to describe the initial sharp growth (until 12 h) and the following dissolution points (t > 12 h), respectively. This fitting makes no assumption as to the final equilibrium concentration.

Table 1. Final Dissolution, D_f, and Dissolution Rate Coefficient, k, are Constants of eq 1 for each evaluated system

System	D_f (μg/L)	k (h^{-1})
H_2O + CuO	61.0 ± 3.5	0.040 ± 0.006
H_2O + [Cho][Asc] + CuO		
H_2O + [Cho][IAA] + CuO	53.5 ± 7.0	0.021 ± 0.007
H_2O + [Cho][IBA] + CuO	67.6 ± 9.9	0.011 ± 0.003
H_2O + [Cho][GA_3] + CuO	123.3 ± 82.4	0.004 ± 0.004
H_2O + [Cho][Sal] + CuO	23763.4 ± 1879.7	0.004 ± 0.001

After 7 days, the dissolution of CuO in water, water + [Cho][IAA], water + [Cho][IBA], or water + [Cho][GA_3] was 61, 55, 58, and 65 μg/L, respectively, indicating that the presence of ILs consisting of PGRs (indole-3-acetic acid, indole-3-butyric acid, and gibberellic acid) did not significantly alter Cu leaching compared with water (Figure 2c−e). However, the dissolution coefficient in water is much higher, indicating faster diffusion of Cu ions from CuO.

With respect to [Cho][IAA], [Cho][IBA], and [Cho]-[GA_3], it is hypothesized that the use of weaker acids as ILs anions such as IAA, IBA, and GA_3 prevents the dissolution of the particles by interacting with the particulate Cu and stabilizing the dispersion of the NM in the solution. In addition, the curve fitting data in Figure 2 by using the shrinking core model indicate that the rate-limiting step in all systems is a chemical reaction. It has been previously shown that the addition of the phytohormone IAA can reduce Cu accumulation in green pea seeds.[27] The use of [Cho][Asc] or [Cho][Sal] resulted in Cu dissolution of 36 and 12 mg/L after 7 days of release (Figure 2b,f), corresponding to 32 and 12% in terms of mass% dissolution, respectively. This may be attributed to the potential of ascorbate and salicylate to dissolve Cu ions by complexation and promote excess [H^+], which in turn could promote the dissolution of more CuO and drive the dissolution process. This has already been demonstrated for malic acid, oxalic acid, succinic acid, and citric acid, which have high binding constants with Cu ions (K_d = [1.299 × 10^4−1.921 × 10^4] M^{-1}).[23] This binding is expected to be stronger when aromatic rings are present in the mixtures,[28] as in the case of equimolar Cu(II) + salicylic acid, where K_d = 2.818 × 10^{10} M^{-1}.[29]

At this point, it is important to emphasize that Cu-based NMs' effectiveness can have dual functionality: at low concentrations, they promote plant growth, while at high

https://doi.org/10.1021/acssusresmgt.4c00041
ACS Sustainable Resour. Manage. 2024, 1, 1291−1301

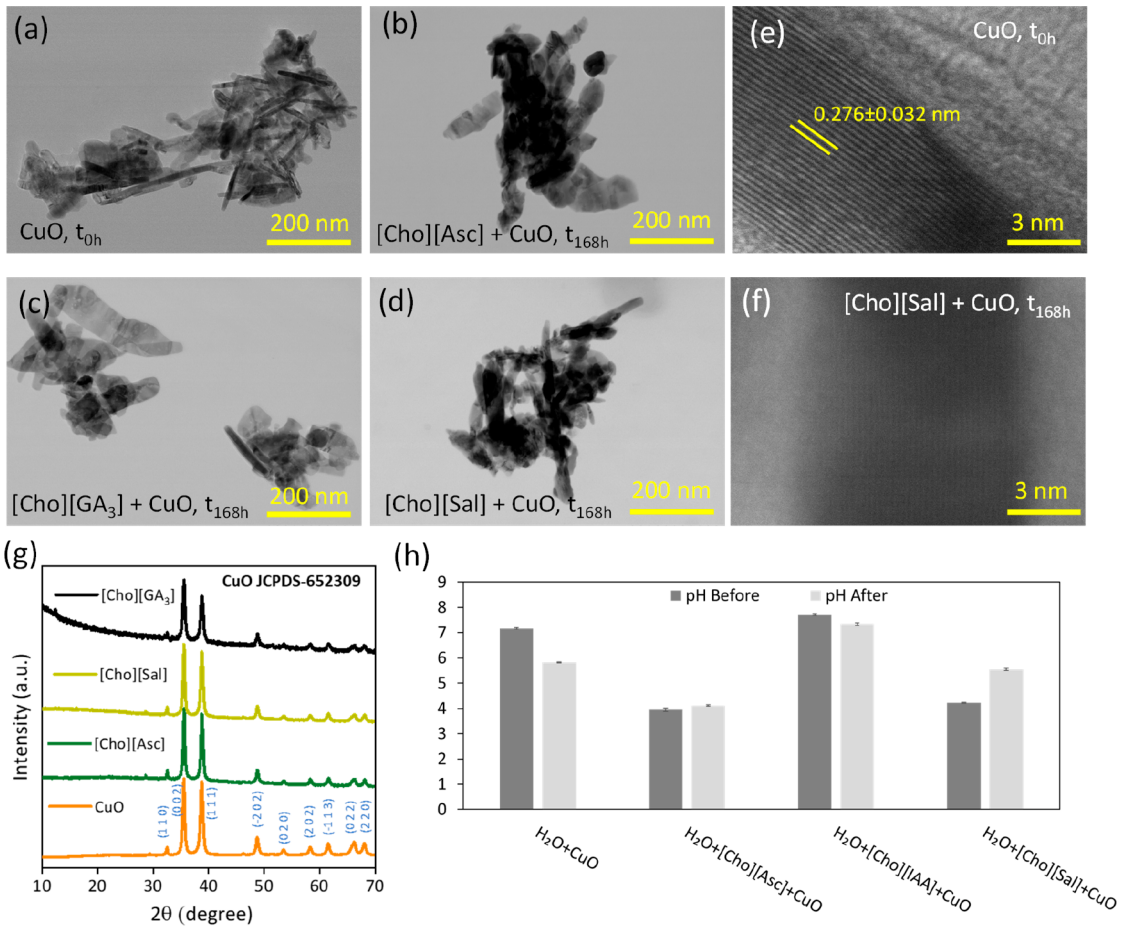

Figure 3. (a) TEM micrograph of CuO before (t_0) adding to PGR-IL solution. (b–d) TEM images of CuO recovered after dissolution experiment (t_{168h}) with aqueous solution of [Cho][Asc], [Cho][GA_3], and [Cho][Sal], respectively. (e and f) High-resolution TEM images showing lattice spacing of CuO before (t_0) and after (t_{168h}) dissolution in [Cho][Sal], respectively. (g) p-XRD patterns of CuO NPs before (t_0) the ion release profile experiments and of non-dissolved CuO after (t_{168h}) the dissolution kinetics in [Cho][Asc], [Cho][GA_3], and [Cho][Sal]-based media. (h) The pH of the investigated media before (t_0) and after (t_{168h}) contact with the CuO NPs. The mean values are significantly different between the samples with $P < 0.05$ as obtained from the paired T-test.

concentrations, they can inhibit overall plant development. That is, when NPs are used as fertilizers, high dissolution of the metal ion may not be desirable, as this may result in it not being used by the plant and therefore accumulating in leaves, soils, and sediments. On the other hand, formulations with higher amounts of dissolved metals can be used to control the growth of unwanted plants, or as pesticides, as has been shown previously.[2,10,30] Hence, understanding the release kinetics of Cu ions from CuO is of paramount importance since it allows fine-tuning of the application of Cu-based NMs in agriculture. Another aspect is the interaction between organic acids and Cu ions, which may reduce or hinder the ability of the plant to absorb the metal ion.[23] In general, the observed different dissolution patterns highlight the importance of both the dissolution and physicochemical properties of NPs for their potential as nanofertilizers. Previous studies have also shown similar results regarding the release of Cu ions from CuO when it was incubated in soil[31] or exposed to different media such as water, sucrose, fumaric acid, or proline,[2,6] as well as when soluble proteins and yeast extract were used.[32]

Effect of PGR-ILs on the Structural Properties of CuO Nanoparticles. The morphology and composition of NMs can directly affect dissolution and subsequent accumulation in plants,[2] making it important to study these variables. Accordingly, TEM (Figure 3a–f) and p-XRD (Figure 3g) techniques were used to characterize the CuO NPs both before and after measuring the ion release kinetics, especially after their exposure to ILs. In addition, the pH of the solutions before (t_0) and after (t_{168h}) contact with the CuO NPs was analyzed (Figure 3h).

Figure 3a shows the TEM image of pristine CuO before the dissolution experiments, which shows the typical defined shape of CuO.[2,6] A similar morphology was observed in the TEM images of CuO after the dissolution experiment with [Cho][Asc], [Cho][GA_3], and [Cho][Sal] (Figure 3b–d). However, the agglomeration of CuO was observed in the presence of [Cho][Asc] and [Cho][Sal]. The aggregation of NPs in the solution prevented measurement of the average size of CuO in the different media. Nevertheless, the distances between atomic layers in CuO and CuO + [Cho][Sal] were evaluated. A total of 25 distances were measured, with dimensions ranging from 0.211 to 0.335 nm. The average sizes are listed in Table S4 and shown in Figure S2. They show almost no difference after contact with the PGR-IL aqueous solution. The EDS mapping of the elements confirmed that the chemical composition of the materials was pure CuO (Figure S3). Using p-XRD analysis (Figure 3g), the original freeze-dried substance was identified as tenorite, a CuO crystal phase,

https://doi.org/10.1021/acssusresmgt.4c00041
ACS Sustainable Resour. Manage. 2024, 1, 1291−1301

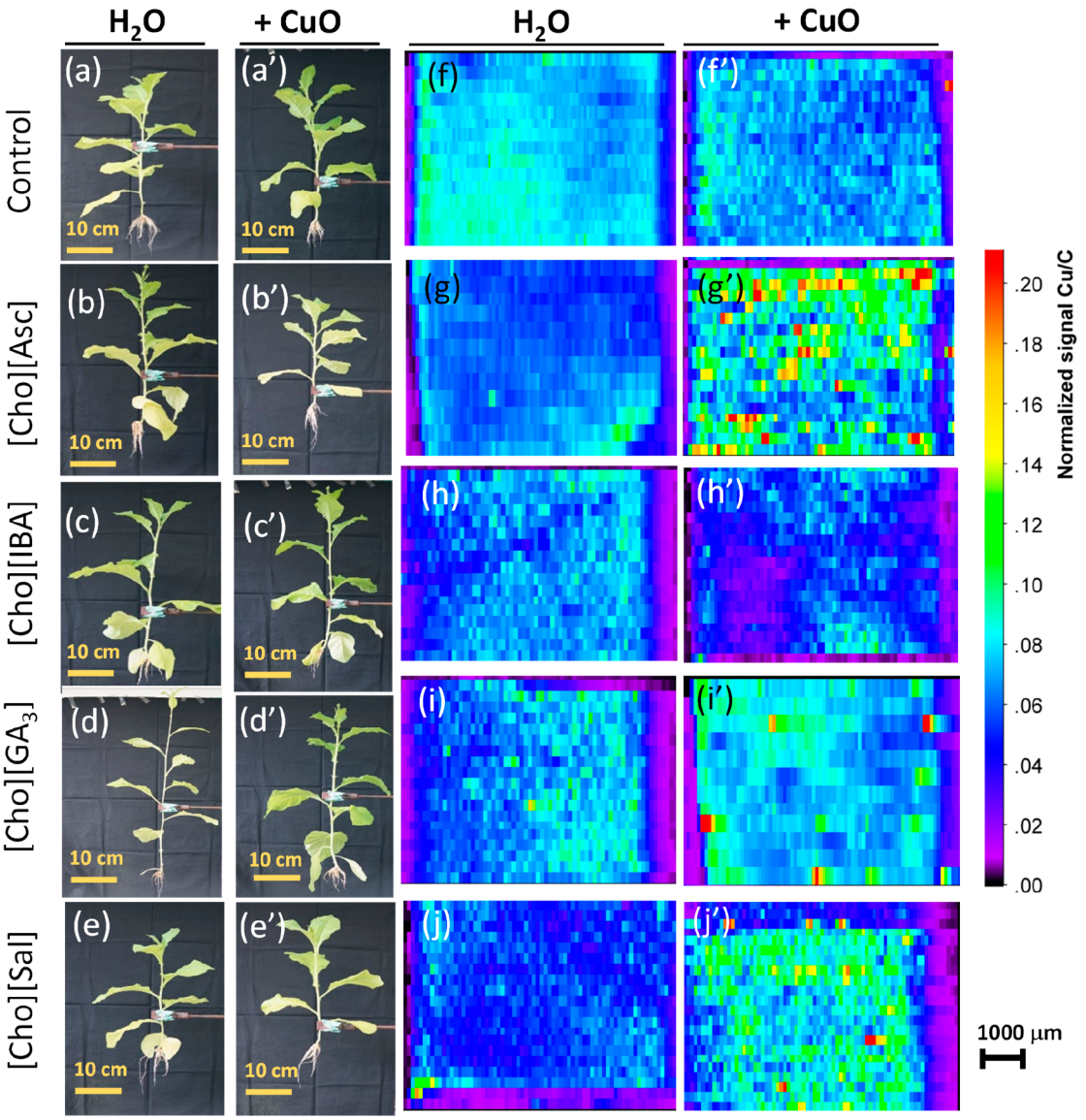

Figure 4. Digital images of *N. tabacum* plants captured at the end of the experiment after treatment with control and aqueous solution of PGR-ILs (a–e) and with water or PGR-IL-modified CuO formulations (a′–e′). Laser ablation inductively coupled plasma mass spectrometry (LA-ICP-MS) 2D mapping images showing the distribution of Cu in the leaf parts obtained at the end of the experiment after treatment with control and aqueous solution of PGR-ILs (f–j) and with water or PGR-IL-modified CuO formulations (f′–j′). The color scale shows the normalized signal of Cu/C.

with a purity of 100%. The crystallite size determined was 24.12 nm, which is consistent with the manufacturer's data. The diffraction peaks in the range from 10° to 70° corresponded precisely to the characteristic Bragg reflections of CuO (JCPDS-652309). Remarkably, no changes or variations in the X-ray angles were observed for the NPs upon exposure to different IL-based media. The results indicate that long-term dissolution and exposure of CuO NPs in the presence of different PGR-ILs do not cause any changes in the morphology and crystallinity of CuO. This indicates that the process is sustainable and allows reuse of the remaining CuO in subsequent batches.

The pH measurements of the PGR-ILs-based solution before and after dissolution are shown in Figure 3h. The nearly neutral and unchanged pH of the aqueous [Cho][IAA] solution contributes to its poor CuO dissolution behavior and results in very low concentrations of dissolved Cu ions. On the other hand, the slightly acidic character of solutions containing [Cho][Asc] or [Cho][Sal] promotes the dissolution of Cu ions, leading to the formation of complexes between Cu ions and the solutions.[33] Similar results were obtained by Borgatta et al.[6] for acidic solutions containing citric acid. After 7 days of experiment, almost no changes in pH are observed, except for the [Cho][Sal]-based solution, where a marginal increase in pH is observed. Since ascorbic acid is an antioxidant and reducing agent that can react with air or light, the ^{1}H NMR spectra of aqueous [Cho][Asc] and [Cho][Asc]+CuO were evaluated after 7 days to look for possible degradation products. As can be seen in Figure S4, minor changes are visible in the ^{1}H NMR spectra of aqueous [Cho][Asc] and [Cho][Asc]+CuO after 7 days kinetics, indicating the absence of additional species in the solution. It is important to note that the reduced quality of the suppressed spectra hinders a more detailed analysis.

Effect of Cu Ions + PGR-ILs Based Nanoformulations on the Growth and Development of *N. tabacum*. As

https://doi.org/10.1021/acssusresmgt.4c00041
ACS Sustainable Resour. Manage. 2024, 1, 1291–1301

mentioned earlier, the use of CuO NPs as nanofertilizers has been investigated for their ability to provide essential micronutrients to plants, leading to various potential benefits such as improved plant growth, higher productivity, and improved resistance to diseases.[2,11,27,34] Considering the different amounts of Cu ions in the different PGR-ILs-based mediums, an application study was conducted to evaluate the impact of such formulations on *N. tabacum* plant growth.

The nanoformulations were sprayed weekly onto leaves by foliar spray in equal amounts per treatment. Treatments included the following: H_2O+CuO, H_2O+[Cho][Asc]+CuO, H_2O+[Cho][IBA]+CuO, H_2O+[Cho][GA_3]+CuO, H_2O +[Cho][Sal]+CuO, and the respective controls (H_2O or H_2O + IL). The foliar spray with increased concentration of the formulation containing [Cho][IBA] was diluted 1000-fold with ultrapure water, in accordance with the suggestion of Skoog,[35] who studied the effect of the concentration of IBA on the growth of excised *Pisum* buds. The amount of Cu ions in the prepared formulations (see the experimental section in the SI) was measured using a total reflectance X-ray fluorescence spectrometer (TXRF) according to the procedure described in the experimental section (see the SI). After 6 days of dissolution, the amounts of Cu ions were 0.041 ± 0.001 mg/L for H_2O+CuO, 34.210 ± 2.630 mg/L for H_2O +[Cho][Asc]+CuO, ~3 μg/L for H_2O+[Cho][IBA]+CuO, 24.386 ± 0.430 mg/L for H_2O+[Cho][GA_3]+CuO, and 22.151 ± 0.585 mg/L for H_2O+[Cho][Sal]+CuO. The stability of all prepared formulations (with and without Cu ions) was investigated after 3 months under room conditions by ^{1}H NMR. The results, as depicted in Figure S5, show only minor changes, which are mainly attributed to the quality of the suppressed spectra. This suggests that the formulations may exhibit stability after 3 months, thereby supporting the possibility of storage under room conditions. However, these results should be interpreted with caution, and further studies employing different techniques will be pursued in the future.

Figure 4a–e shows digital images of tobacco plants taken at harvest showing their appearance after spraying with water and various aqueous solutions of PGR-ILs. In contrast, Figure 4a′–e′ shows the digital images of plants treated with CuO+H_2O or CuO+PGR-ILs+H_2O. Plants subjected to PGR-ILs showed minor changes in growth characteristics compared to plants treated with pure water or an aqueous solution of PGR-ILs. Root system architecture was unaffected in all of the treatments. In particular, the use of IL [Cho][GA_3], both with and without Cu ions in the solution, resulted in the development of tall and slender plants (Figure 4d,d′). On the other hand, based on qualitative observations, treatments with higher concentrations of Cu ions, such as H_2O+[Cho]-[Asc]+CuO and H_2O+[Cho][Sal]+CuO, showed lower plant growth (Figure 4b,b′ and Figure 4e,e′). Plants treated with H_2O+[Cho][IBA]+CuO (containing the least Cu ions) grew slightly longer and maintained a healthy appearance (Figure 4c,c′).

To investigate the impact of CuO+PGR-ILs nanoformulations on micronutrient uptake, we performed LA-ICP-MS analyses of leaf sections (Figure 4f–j) and estimated the concentration of Cu ions in leaves using TXRF (Figure 5). Figure 4f–j shows LA-ICP-MS images of tobacco leaf sections treated with various aqueous solutions, including water and different PGR-ILs. Figure 4f′–j′ shows LA-ICP-MS 2D mapping images of plants treated with CuO+H_2O or CuO +PGR-ILs+H_2O. It can be seen from Figure 4f–j that a very

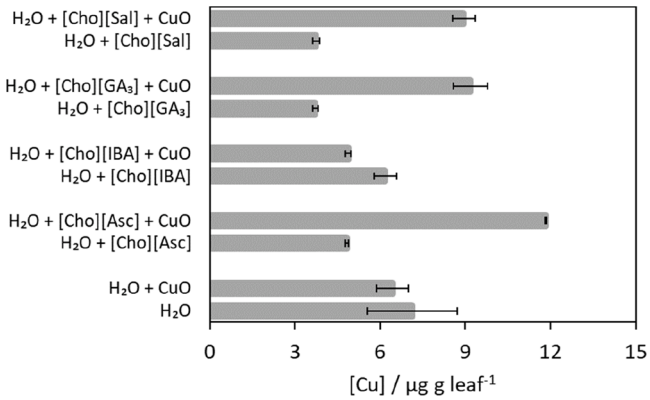

Figure 5. Leaf Cu content obtained after harvesting and analyzed by total reflectance X-ray fluorescence spectrometry. The mean values are significantly different between the different treatments with P <0.05 as obtained from the paired T-test.

low Cu/C signal is observed, which can be attributed to the absence of Cu ions in these treatments. Similar observations were made for treatments with minimal Cu ion concentrations, such as CuO+H_2O (Figure 4f′) or CuO+[Cho][IBA]+H_2O (Figure 4h′). Conversely, formulations with higher concentrations of Cu ions resulted in greater accumulation of Cu in the leaves, as indicated by significantly higher Cu/C signals. This effect is particularly evident when using [Cho][Asc] (Figure 4g′), [Cho][GA_3] (Figure 4i′), and [Cho][Sal] (Figure 4j′), which are ILs that enhance the dissolution of CuO. TXRF analysis of Cu ions in the leaves of tobacco plants obtained after harvest reflected the trend of LA-ICP-MS mapping of Cu ions in the different treatments (Figure 5). Overall, Cu mapping by LA-ICP-MS and Cu analysis by TXRF showed that the formulations containing [Cho][Asc], [Cho]-[GA_3], and [Cho][Sal] released more Cu to the plant leaves, highlighting the importance of the dissolution profile for leaf-surface interactions and micronutrient uptake.

Recognizing that the amount of Cu ions affects the uptake of micronutrients and promotion of tobacco plant growth, we then investigated how those affect the growth characteristics, physiological status, CO_2 uptake, and crude protein content of tobacco plants. Figure 6a shows the leaf area of tobacco plants treated with different formulations. Interestingly, the leaf area was larger in all treatments without Cu ions, except for the treatment with CuO+[Cho][Sal]+H_2O. On the other hand, leaf chlorophyll index (CI) values were higher in all treatments with CuO-based formulations (Figure 6b). The treatments with low Cu ion concentrations, such as CuO+H_2O and CuO +[Cho][IBA]+H_2O, showed higher CI. On the other hand, the use of ILs based on [Cho][Asc], [Cho][GA_3], and [Cho][Sal] resulted in higher dissolution of CuO but not in higher CI. These findings are consistent with the observations presented in Figures 4 and 5.

Results on gas exchange parameters such as the net photosynthetic rate (P_N) (Figure 6c), leaf transpiration (T_r) (Figure 6d), and stomata conductance (Figure 6e) indicate significant changes due to the inclusion of CuO in the formulations. However, the results of the intercellular CO_2 concentration (Ci) were not significant between the different formulations with and without CuO. The highest P_N was obtained with the formulation containing lower Cu ion concentrations (CuO+[Cho][IBA]+H_2O), which agrees well with the higher chlorophyll index data. Overall, foliar

https://doi.org/10.1021/acssusresmgt.4c00041
ACS Sustainable Resour. Manage. 2024, 1, 1291–1301

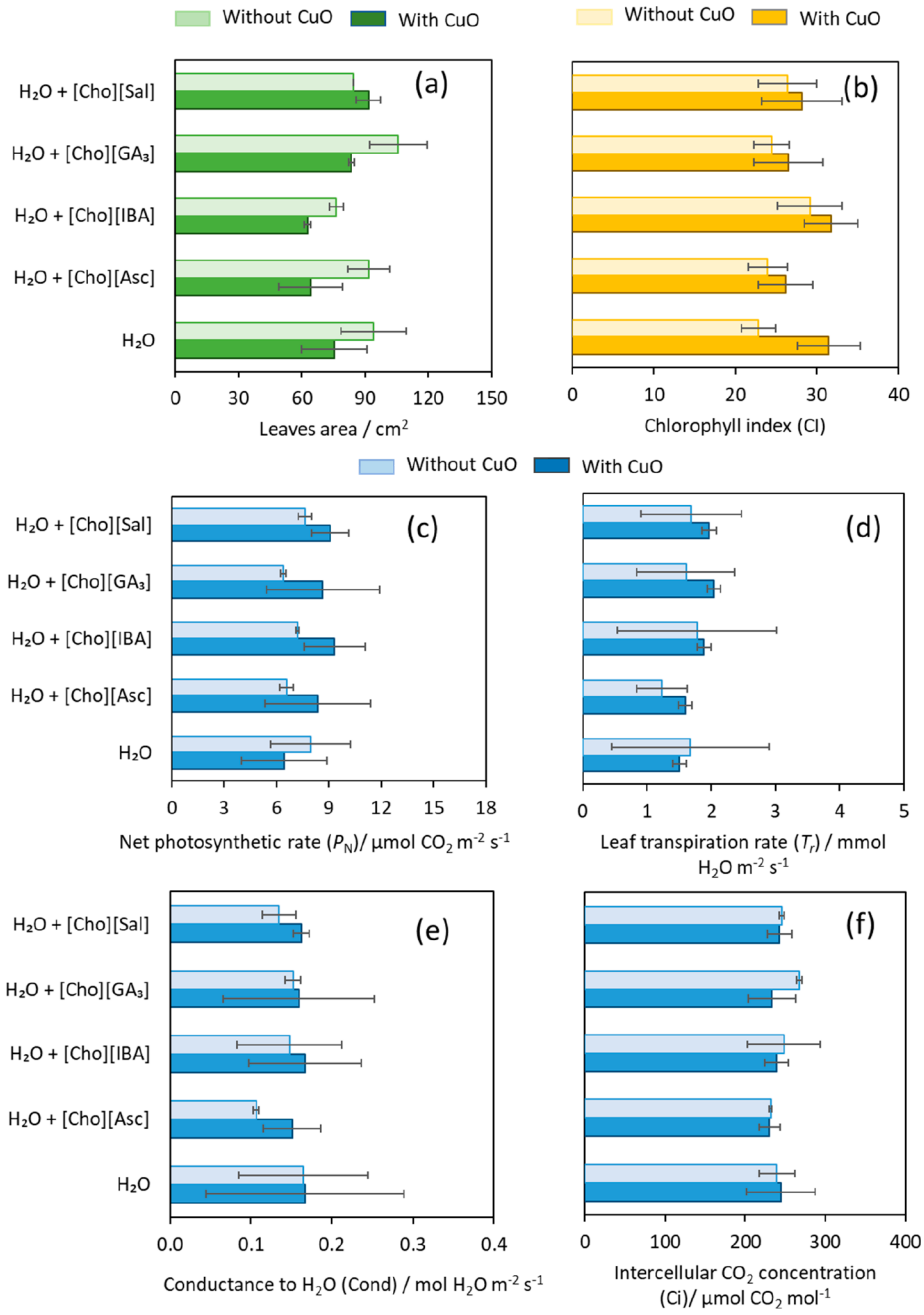

Figure 6. Effect of different treatments on the leaf area (a), chlorophyll index (b), net photosynthetic rate (c), leaf transpiration rate (d), conductance to H_2O (e), and intercellular CO_2 concentration (f). The mean values for panels a, b, and f are significantly different between the different treatments with P <0.05 as obtained from the paired T-test.

application of CuO-based NMs modified with PGR-ILs significantly affects the phenotype, physiological parameters, and photosynthetic rate of *N. tabacum* plants. The activity can be correlated to PGR-IL, which determines the concentration of Cu ions in the solution.

The increase in P_N in the treatments with low Cu ion concentrations, such as CuO+H_2O and CuO+[Cho]-[IBA]+H_2O, resulted in an increase in the overall plant length (root + above soil) (Figure 7a) and higher dry biomass accumulation (Figure 7b). This indicates that there was a higher level of assimilation of photosynthetic carbon in the plant parts. In contrast, it was observed that treatments with a higher concentration of Cu ions resulted in a decrease in the plant length and dry biomass yield. A similar trend was observed in the amount of CO_2 sequestered per plant (Figure 7c), where treatments with lower concentrations of Cu ions had 20−30% higher CO_2 sequestration capacity compared to the other treatments. The crude protein content per plant was higher in all treatments with CuO than in the corresponding aqueous formulations (Figure 7d). However, a significant difference was observed in the formulation with a low Cu ion concentration. Overall, the above results suggest that the dissolution of CuO plays a crucial role in considering its potential as a sustainable nanofertilizer.

This study acknowledges the potential of Cu-based NMs in the suppression of plant infections. The amounts of Cu dissolved in the nanoformulations applied ranged from ∼3 µg/L for H_2O+[Cho][IBA]+CuO to around 34.2 mg/L for H_2O

https://doi.org/10.1021/acssusresmgt.4c00041
ACS Sustainable Resour. Manage. 2024, 1, 1291−1301

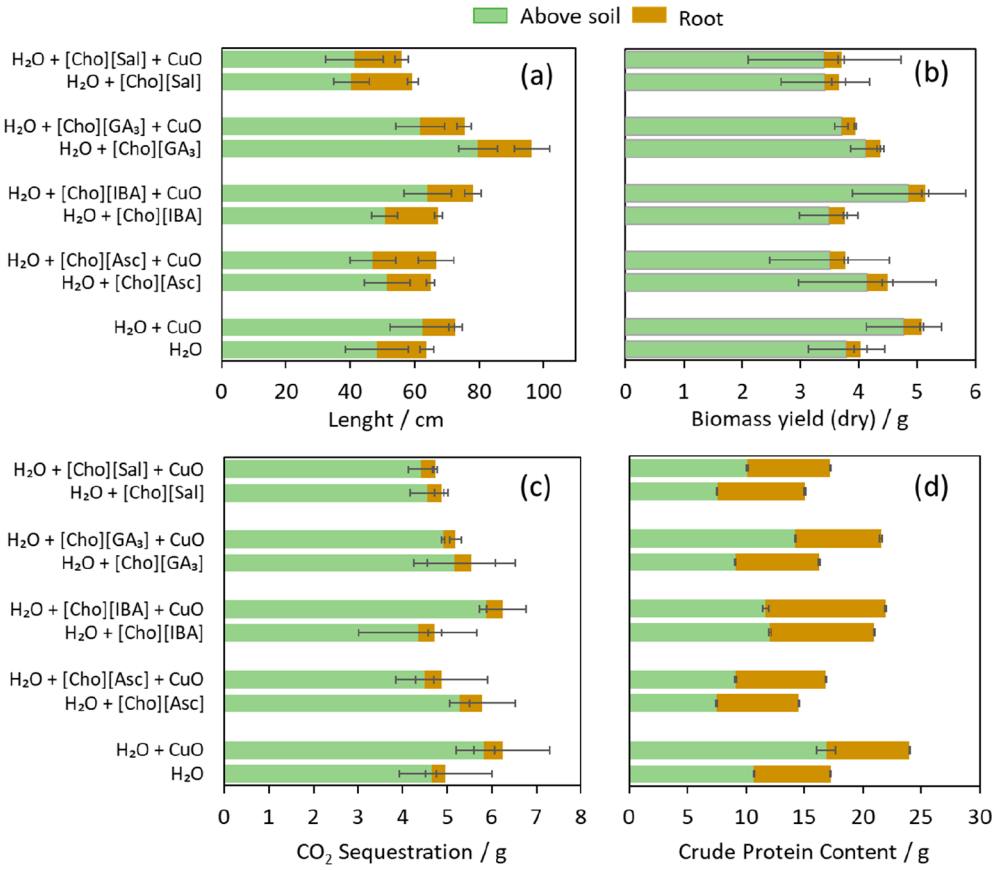

Figure 7. Effect of different treatments on full length (a), dry biomass yield (b), CO_2 sequestration (c), and crude protein content (d) per plant. The mean values are significantly different between the different treatments with $P < 0.05$ as obtained from the paired T-test.

+[Cho][Asc]+CuO. Drawing a comparison with relevant studies, Borgatta et al.[6] demonstrated that foliar exposure of watermelon to $Cu_3(PO_4)_2$ nanosheets at a concentration of 10 mg/L effectively suppressed *Fusarium* infection. Additionally, CuO NPs exhibited similar impacts but at much higher concentrations ranging from 250 to 1000 mg/L. Subsequent research by Ma et al.[2] revealed that *Fusarium virguliforme* infection significantly reduced soybean shoot mass and that the foliar application of CuO nanosheets at 50 and 250 mg/L alleviated much of the damage. Both cited works emphasize the importance of particle characteristics, such as morphology, coordination environment, and dissolution profile, as crucial determinants of the plant's response. The concentration range of Cu ions in the nanoformulations in this study falls within the effective range identified in previous research, suggesting the potential efficacy of the applied nanoformulations in suppressing plant infections while highlighting the importance of particle characteristics in influencing outcomes.

Ecological Footprint. Cu plays a crucial role in disease prevention as an essential micronutrient in agriculture.[11,20] However, the excessive use of Cu in large quantities has raised concerns about its possible accumulation in the environment. Moreover, Cu is considered a strategic raw material whose availability is limited, posing a risk to the future supply. As previously stated, CuO-based nanofertilizers can be an alternative delivery system for nanoscale Cu that could be useful in controlling plant diseases and increasing the productivity. CuO nanofertilizers applied to leaves have been shown to control sudden death syndrome.[2] They also provide protection to plants against pathogens by increasing the expression of the polyphenol oxidase gene.[36] In addition, foliar application of CuO was found to increase the overall biomass and fruit yield of tomato and eggplant.[11] Nevertheless, it is important to note that nanofertilizers are large-volume agrochemicals whose limited uptake by plants can lead to significant accumulation of metal ions in the environment, resulting in the loss of micronutrients. Therefore, improving the efficiency of fertilizer use is critical for sustainable and environmentally friendly agriculture. As discussed above, the dissolution rate of CuO is affected by its amalgamation with non-toxic and biocompatible PGR-ILs. Moreover, greenhouse experiments conducted using a CuO+PGR-ILs-based nanoformulation and tobacco as a model plant have demonstrated the ability of PGR-ILs to influence overall plant growth and control the amount of Cu ions. These results highlight the potential of PGR-ILs to control the release of Cu ions in nanoformulation, with long-term benefits for plant development, enhanced CO_2 sequestration, and environmental sustainability. Furthermore, the integration of nanotechnology and ILs into agricultural practices has the potential to contribute to sustainable and efficient food production systems, while minimizing the use of conventional chemical fertilizers and pesticides. The future of PGR-ILs-based nanoformulations holds great promise in agricultural innovation due to PGR-ILs' unique properties and availability, sourced from natural products and biomass, ensuring sustainability. Moreover, their scalable synthesis and customization make them suitable for various crops, allowing mass production for large-scale agriculture.

https://doi.org/10.1021/acssusresmgt.4c00041
ACS Sustainable Resour. Manage. 2024, 1, 1291−1301

CONCLUSIONS

Understanding how NPs dissolve in exposure media is critical to classifying their hazard potential and determining their fate in a living system. In this study, the release of Cu ions from CuO NPs was investigated in aqueous solutions containing ILs from biomolecules based on PGRs. The dissolution kinetics results show that [Cho][Asc] and [Cho][Sal] ILs significantly increase the release of Cu ions in water (200- to 700-fold higher than those of the control and other PGR ILs) without affecting the NP structure. On the other hand, the use of [Cho][IAA], [Cho][IBA], and [Cho][GA_3] does not significantly change the Cu dissolution compared to water but significantly decreases the dissolution rate, indicating slower diffusion. In addition, the effects of foliar application of Cu-based nanoformulations with PGR-ILs on *N. tabacum* plants in a greenhouse were investigated. Cu mapping by LA-ICP-MS and Cu ion analysis by TXRF showed that formulations containing [Cho][Asc], [Cho][GA_3], and [Cho][Sal] led to a higher amount of Cu in the plant tissue. This highlights the importance of controlling the dissolution in leaf-surface interactions and plant response. The application of CuO +PGR-ILs nanoformulations affected the plant phenotype, physiological parameters, photosynthetic rate, and CO_2 sequestration. The activity was found to correlate with the PGR-ILs used, which determined the amount of Cu ions in the solution. Based on these results, we emphasize the importance of using small quantities of nanoscale CuO+PGR-IL-based formulations as fertilizers by foliar application. These results provide valuable insights for the development of NM-based plant nanochemicals, which are crucial in the field of plant nanotechnology for enhancing crop productivity. Considering the bifunctional effect of Cu NPs as plant growth promoter (at low concentration of Cu NPs) and crop protection agent (at high concentration of Cu NPs), a future study aims to investigate the advantage of high CuO dissolution kinetics of [Cho][Asc] and [Cho][Sal] in plants under biotic or abiotic stress.

ASSOCIATED CONTENT

Supporting Information

The Supporting Information is available free of charge at https://pubs.acs.org/doi/10.1021/acssusresmgt.4c00041.

Detailed Experimental Section, experimental ^{1}H NMR spectra for all precursors and synthesized ionic liquids, information on the suspensions' preparation; ion release profiles tables, and NPs characterization data (PDF)

AUTHOR INFORMATION

Corresponding Authors

Gregory Franklin − *Institute of Plant Genetics of the Polish Academy of Sciences, 60-479 Poznan, Poland;* orcid.org/0000-0002-6745-3528; Email: fgre@igr.poznan.pl

Dibyendu Mondal − *Institute of Plant Genetics of the Polish Academy of Sciences, 60-479 Poznan, Poland; Centre for Nano and Material Sciences, Jain (Deemed-to-be University), Bangalore, Karnataka 562112, India;* orcid.org/0000-0002-1715-5514; Email: dmon@igr.poznan.pl, m.dibyendu@jainuniversity.ac.in

Authors

Mónia A. R. Martins − *Institute of Plant Genetics of the Polish Academy of Sciences, 60-479 Poznan, Poland; Centro de Investigação de Montanha (CIMO) and Laboratório para a Sustentabilidade e Tecnologia em Regiões de Montanha, Instituto Politécnico de Bragança, 5300-253 Bragança, Portugal;* orcid.org/0000-0003-0748-1612

Leonard M. Kiirika − *Institute of Plant Genetics of the Polish Academy of Sciences, 60-479 Poznan, Poland*

Nicolas Schaffer − *CICECO − Aveiro Institute of Materials, University of Aveiro, 3810-193 Aveiro, Portugal;* orcid.org/0000-0002-0747-2532

Adam Sajnóg − *Department of Trace Analysis, Adam Mickiewicz University, 61-614 Poznań, Poland*

João A. P. Coutinho − *CICECO − Aveiro Institute of Materials, University of Aveiro, 3810-193 Aveiro, Portugal;* orcid.org/0000-0002-3841-743X

Complete contact information is available at: https://pubs.acs.org/10.1021/acssusresmgt.4c00041

Notes

The authors declare no competing financial interest.

ACKNOWLEDGMENTS

This work was supported by the NANOPLANT project, which received funding from the European Union's Horizon 2020 research and innovation program under grant agreement no. 856961. Additionally, this work was partly developed within the scope of the project CICECO-Aveiro Institute of Materials, UIDB/50011/2020, UIDP/50011/2020, and LA/P/0006/2020, financed by national funds through the FCT/MEC (PIDDAC). The NMR spectrometers are part of the National NMR Network (PTNMR) and are partially supported by Infrastructure Project No. 022161 (co-financed by FEDER through COMPETE 2020, POCI and PORL and FCT through PIDDAC). The authors would like to thank Robin Schmid (University of Münster) for providing the ImaJar software.

REFERENCES

(1) White, J. C.; Gardea-Torresdey, J. Achieving Food Security through the Very Small. *Nat. Nanotechnol.* **2018**, *13* (8), 627−629.

(2) Ma, C.; Borgatta, J.; Hudson, B. G.; Tamijani, A. A.; De La Torre-Roche, R.; Zuverza-Mena, N.; Shen, Y.; Elmer, W.; Xing, B.; Mason, S. E.; Hamers, R. J.; White, J. C. Advanced Material Modulation of Nutritional and Phytohormone Status Alleviates Damage from Soybean Sudden Death Syndrome. *Nat. Nanotechnol.* **2020**, *15* (12), 1033−1042.

(3) Kah, M.; Tufenkji, N.; White, J. C. Nano-Enabled Strategies to Enhance Crop Nutrition and Protection. *Nat. Nanotechnol.* **2019**, *14* (6), 532−540.

(4) Servin, A. D.; White, J. C. Nanotechnology in Agriculture: Next Steps for Understanding Engineered Nanoparticle Exposure and Risk. *NanoImpact* **2016**, *1*, 9−12.

(5) Dordas, C. Role of Nutrients in Controlling Plant Diseases in Sustainable Agriculture. A Review. *Agron. Sustain. Dev.* **2008**, *28* (1), 33−46.

(6) Borgatta, J.; Ma, C.; Hudson-Smith, N.; Elmer, W.; Plaza Pérez, C. D.; De La Torre-Roche, R.; Zuverza-Mena, N.; Haynes, C. L.; White, J. C.; Hamers, R. J. Copper Based Nanomaterials Suppress Root Fungal Disease in Watermelon (Citrullus Lanatus): Role of Particle Morphology, Composition and Dissolution Behavior. *ACS Sustain. Chem. Eng.* **2018**, *6* (11), 14847−14856.

(7) Dimkpa, C. O.; Bindraban, P. S. Fortification of Micronutrients for Efficient Agronomic Production: A Review. *Agron. Sustain. Dev.* **2016**, *36* (1), 7.

(8) Hoang, T. C.; Rogevich, E. C.; Rand, G. M.; Gardinali, P. R.; Frakes, R. A.; Bargar, T. A. Copper Desorption in Flooded Agricultural Soils and Toxicity to the Florida Apple Snail (Pomacea

Paludosa): Implications in Everglades Restoration. *Environ. Pollut.* **2008**, *154* (2), 338−347.
(9) Nunes, I.; Jacquiod, S.; Brejnrod, A.; Holm, P. E.; Johansen, A.; Brandt, K. K.; Priemé, A.; Sørensen, S. J. Coping with Copper: Legacy Effect of Copper on Potential Activity of Soil Bacteria Following a Century of Exposure. *FEMS Microbiol. Ecol.* **2016**, *92* (11), fiw175.
(10) Servin, A.; Elmer, W.; Mukherjee, A.; De la Torre-Roche, R.; Hamdi, H.; White, J. C.; Bindraban, P.; Dimkpa, C. A Review of the Use of Engineered Nanomaterials to Suppress Plant Disease and Enhance Crop Yield. *J. Nanoparticle Res.* **2015**, *17* (2), 92.
(11) Elmer, W. H.; White, J. C. The Use of Metallic Oxide Nanoparticles to Enhance Growth of Tomatoes and Eggplants in Disease Infested Soil or Soilless Medium. *Environ. Sci. Nano* **2016**, *3* (5), 1072−1079.
(12) Wu, H.; Li, Z. Nano-Enabled Agriculture: How Do Nanoparticles Cross Barriers in Plants? *Plant Commun.* **2022**, *3* (6), 100346.
(13) Zhao, L.; Hu, Q.; Huang, Y.; Keller, A. A. Response at Genetic, Metabolic, and Physiological Levels of Maize (Zea Mays) Exposed to a Cu(OH) 2 Nanopesticide. *ACS Sustain. Chem. Eng.* **2017**, *5* (9), 8294−8301.
(14) Mitter, N.; Worrall, E. A.; Robinson, K. E.; Li, P.; Jain, R. G.; Taochy, C.; Fletcher, S. J.; Carroll, B. J.; Lu, G. Q.; Xu, Z. P. Clay Nanosheets for Topical Delivery of RNAi for Sustained Protection against Plant Viruses. *Nat. Plants* **2017**, *3* (2), 16207.
(15) Hu, P.; An, J.; Faulkner, M. M.; Wu, H.; Li, Z.; Tian, X.; Giraldo, J. P. Nanoparticle Charge and Size Control Foliar Delivery Efficiency to Plant Cells and Organelles. *ACS Nano* **2020**, *14* (7), 7970−7986.
(16) Lopez-Lima, D.; Mtz-Enriquez, A. I.; Carrión, G.; Basurto-Cereceda, S.; Pariona, N. The Bifunctional Role of Copper Nanoparticles in Tomato: Effective Treatment for Fusarium Wilt and Plant Growth Promoter. *Sci. Hortic. (Amsterdam).* **2021**, *277*, 109810.
(17) Rogers, R. D.; Seddon, K. R. Chemistry. Ionic Liquids-Solvents of the Future? *Science* **2003**, *302* (5646), 792−793.
(18) Haron, G. A. S.; Mahmood, H.; Noh, M. H.; Alam, M. Z.; Moniruzzaman, M. Ionic Liquids as a Sustainable Platform for Nanocellulose Processing from Bioresources: Overview and Current Status. *ACS Sustain. Chem. Eng.* **2021**, *9* (3), 1008−1034.
(19) Mondal, D.; Sharma, M.; Mukesh, C.; Gupta, V.; Prasad, K. Improved Solubility of DNA in Recyclable and Reusable Bio-Based Deep Eutectic Solvents with Long-Term Structural and Chemical Stability. *Chem. Commun.* **2013**, *49* (83), 9606−9608.
(20) Marmiroli, M.; Pagano, L.; Rossi, R.; De La Torre-Roche, R.; Lepore, G. O.; Ruotolo, R.; Gariani, G.; Bonanni, V.; Pollastri, S.; Puri, A.; Gianoncelli, A.; Aquilanti, G.; D'Acapito, F.; White, J. C.; Marmiroli, N. Copper Oxide Nanomaterial Fate in Plant Tissue: Nanoscale Impacts on Reproductive Tissues. *Environ. Sci. Technol.* **2021**, *55* (15), 10769−10783.
(21) Pateli, I. M.; Thompson, D.; Alabdullah, S. S. M.; Abbott, A. P.; Jenkin, G. R. T.; Hartley, J. M. The Effect of PH and Hydrogen Bond Donor on the Dissolution of Metal Oxides in Deep Eutectic Solvents. *Green Chem.* **2020**, *22* (16), 5476−5486.
(22) Elder, S. H.; DiSalvo, F. J.; Topor, L.; Navrotsky, A. Thermodynamics of Ternary Nitride Formation by Ammonolysis: Application to Lithium Molybdenum Nitride (LiMoN2), Sodium Tungsten Nitride (Na3WN3), and Sodium Tungsten Oxide Nitride (Na3WO3N). *Chem. Mater.* **1993**, *5* (10), 1545−1553.
(23) Huang, Y.; Zhao, L.; Keller, A. A. Interactions, Transformations, and Bioavailability of Nano-Copper Exposed to Root Exudates. *Environ. Sci. Technol.* **2017**, *51* (17), 9774−9783.
(24) Misra, S. K.; Dybowska, A.; Berhanu, D.; Croteau, M. N.; Luoma, S. N.; Boccaccini, A. R.; Valsami-Jones, E. Isotopically Modified Nanoparticles for Enhanced Detection in Bioaccumulation Studies. *Environ. Sci. Technol.* **2012**, *46* (2), 1216−1222.
(25) Dialysis tubing cellulose membrane avg. flat width 10 mm (0.4 in.); Sigma-Aldrich. https://www.sigmaaldrich.com/PT/en/product/sigma/d9277 (accessed Feb 5, 2023).
(26) Chakraborty, S.; Nair, A.; Paliwal, M.; Dybowska, A.; Misra, S. K. Exposure Media a Critical Factor for Controlling Dissolution of CuO Nanoparticles. *J. Nanoparticle Res.* **2018**, *20* (12), 331.
(27) Ochoa, L.; Zuverza-Mena, N.; Medina-Velo, I. A.; Flores-Margez, J. P.; Peralta-Videa, J. R.; Gardea-Torresdey, J. L. Copper Oxide Nanoparticles and Bulk Copper Oxide, Combined with Indole-3-Acetic Acid, Alter Aluminum, Boron, and Iron in Pisum Sativum Seeds. *Sci. Total Environ.* **2018**, *634*, 1238−1245.
(28) Yamauchi, O.; Odani, A. Structure-Stability Relationship in Ternary Copper(II) Complexes Involving Aromatic Amines and Tyrosine or Related Amino Acids. Intramolecular Aromatic Ring Stacking and Its Regulation through Tyrosine Phosphorylation. *J. Am. Chem. Soc.* **1985**, *107* (21), 5938−5945.
(29) Abbasi, S. A.; Sharma, R. K. Copper Salicylates: Occurrence of Linear Free Energy Relationships. *J. Inorg. Nucl. Chem.* **1981**, *43* (3), 625−627.
(30) Zeng, Q.; Yu, C.; Chang, X.; Wan, Y.; Ba, Y.; Li, C.; Lv, H.; Guo, Z.; Cai, T.; Ren, Z.; Qin, Y.; Zhang, Y.; Ma, K.; Li, J.; He, S.; Wan, H. CeO2 Nanohybrid as a Synergist for Insecticide Resistance Management. *Chem. Eng. J.* **2022**, *446*, 137074.
(31) Gao, X.; Avellan, A.; Laughton, S.; Vaidya, R.; Rodrigues, S. M.; Casman, E. A.; Lowry, G. V. CuO Nanoparticle Dissolution and Toxicity to Wheat (Triticum Aestivum) in Rhizosphere Soil. *Environ. Sci. Technol.* **2018**, *52* (5), 2888−2897.
(32) Gunawan, C.; Teoh, W. Y.; Marquis, C. P.; Amal, R. Cytotoxic Origin of Copper(II) Oxide Nanoparticles: Comparative Studies with Micron-Sized Particles, Leachate, and Metal Salts. *ACS Nano* **2011**, *5* (9), 7214−7225.
(33) Ko, C. K.; Lee, W. G. Effects of PH Variation in Aqueous Solutions on Dissolution of Copper Oxide. *Surf. Interface Anal.* **2010**, *42* (6-7), 1128−1130.
(34) Huang, G.; Zuverza-Mena, N.; White, J. C.; Hu, H.; Xing, B.; Dhankher, O. P. Simultaneous Exposure of Wheat (Triticum Aestivum L.) to CuO and S Nanoparticles Alleviates Toxicity by Reducing Cu Accumulation and Modulating Antioxidant Response. *Sci. Total Environ.* **2022**, *839*, 156285.
(35) Skoog, F. Experiments on Bud Inhibition with Indole-3-Acetic Acid. *Am. J. Bot.* **1939**, *26* (9), 702.
(36) Elmer, W.; De La Torre-Roche, R.; Pagano, L.; Majumdar, S.; Zuverza-Mena, N.; Dimkpa, C.; Gardea-Torresdey, J.; White, J. C. Effect of Metalloid and Metal Oxide Nanoparticles on Fusarium Wilt of Watermelon. *Plant Dis.* **2018**, *102* (7), 1394−1401.

https://doi.org/10.1021/acssusresmgt.4c00041
ACS Sustainable Resour. Manage. 2024, 1, 1291−1301